



Wall Smoke Deposition from a Hot Smoke Layer

*Siamak Riahi**, Department of Civil and Environmental Engineering, The George Washington University, Phillips Hall, Room 643 The Academic Center, 801 22nd Street, NW, Washington, DC 20052, USA

Craig L. Beyler, Hughes Associates, 3610 Commerce Drive, Suite 817, Baltimore, MD 21227, USA

JudithAnn Hartman, Chemistry Department, U.S. Naval Academy, 572 M Holloway Road, Annapolis, MD 21402-5026, USA

Received: 26 September 2011/**Accepted:** 16 May 2012

Abstract. Smoke deposition from a hot smoke layer onto wall surfaces was studied in a hood apparatus using polymethylmethacrylate, polypropylene, and gasoline as fuels. Based upon prior analysis by Butler and Mulholland, the smoke deposition was expected to be dominated by thermophoresis. The deposited smoke samples were collected on glass filter paper attached to the hood wall and the mass per unit area of smoke deposited was measured gravimetrically. Measurements were made of quantities required for the prediction of thermophoretic smoke deposition. The smoke deposition measured in the experimental program was well predicted by the thermophoretic smoke deposition equation. The thermophoretic smoke deposition equation was found to be suitable for predicting smoke deposition onto wall surfaces exposed to fire environments.

Keywords: Smoke, Deposition, Thermophoresis

1. Background

Flaming fires generate smoke particles as a result of incomplete combustion. The primary particles are spheres of approximately 30 nm diameter and the long chain agglomerates are between 100 nm and 10,000 nm (0.1 μm to 10 μm) [1]. The term smoke in this work is defined as the smoke aerosol or condensed phase component of the products of combustion. While smokes can be dominated by liquid aerosols (e.g. smoldering fires and flaming wood fires), the smokes studied here were black carbonaceous smokes typical of flaming fires.

Smoke deposition is the process in which smoke particles collect on solid surfaces. This process will decrease the concentration of smoke in the gas since particles are lost to the surface. Smoke deposition is of significance with respect to the creation of property damage, slowing smoke detection, and forensic smoke

* Correspondence should be addressed to: Siamak Riahi, E-mail: sriahi@gwmail.gwu.edu

pattern analysis. Five smoke deposition mechanisms have been identified in fire: thermophoresis, diffusion, sedimentation, inertial impaction, and turbulent diffusion [1]. Based upon the analysis of Butler and Mulholland [1], smoke deposition on wall surfaces exposed to fire environments is expected to be dominated by thermophoresis.

Thermophoresis is the transport of smoke particles by a thermal gradient. Thus, thermophoretic smoke deposition occurs as a direct result of convection heat transfer to a surface. A common example of thermophoretic smoke deposition is the blackening of a cold metal knife immersed in a candle flame. The temperature gradient established between the flame and the metal knife drives the carbon particles produced in the combustion process towards the knife, where they deposit.

Most research in the area of smoke has been focused on smoke as a dispersion of particles in the air that obscures vision [2]. Butler and Mulholland reviewed the characteristics of smoke aerosols in fire [1]. They present the current state of knowledge about smoke aerosol phenomena that affect smoke toxicity: smoke generation, fractal structure of smoke, smoke deposition via thermophoresis, sedimentation, and diffusion, and smoke agglomerate growth through coagulation and condensation. Ciro et al. [3] used a thermophoretic smoke deposition model based on previous analytical works [4, 5] to successfully predict smoke deposition on a cold rod placed in a pool fire. In Ciro's work, smoke deposition was sufficiently large that the physical thickness of the deposited layer could be measured directly. However, in most cases of interest the smoke deposition, the deposited layer is sufficiently thin that cannot be readily measured.

Computer fire models have not taken smoke deposition into account. Gottuk et al. [6] showed that smoke deposition in the plume impingement area and the ceiling jet was up to 40% of the smoke produced by the fire. This was found to substantially affect the gas phase optical density in the ceiling jet and the response of smoke detectors. Hamins et al. [7] found that predictions of optical density using FDS were consistently high (over 35%). Floyd [8] developed thermophoretic and turbulent diffusion smoke deposition models within FDS and performed trial calculations of these experiments which achieved better agreement with the data [9].

The goal of the present work is to develop methods for quantifying smoke deposition and use these methods to validate a thermophoretic model of smoke deposition on wall surfaces. The smoke deposition measurement method developed is gravimetric measurements on glass filter paper pinned to the wall surface. The gravimetric method provides a direct measurement of smoke deposition. The experimental program was carried out in a hood apparatus in which a hot smoke layer was formed. Measurements required to predict thermophoretic smoke deposition were implemented in the hood apparatus. The apparatus is described in the following section. The smoke deposition results and comparisons with the thermophoretic model are presented subsequently.

2. Experimental Apparatus

The hood apparatus was designed to collect the hot smoke layer produced by a burning fuel sample [10]. The hood apparatus consisted of a steel frame ($0.6\text{ m} \times 0.6\text{ m} \times 0.9\text{ m}$ high) with walls of inorganic fibreboard (see Figure 1). Thermal conductivity of the fibreboard material varies from 0.06 to 0.18 W/m K for the temperature range of 400°C to $1,000^\circ\text{C}$ [11]. An exhaust plenum on the right side of the main chamber ($0.45\text{ m} \times 0.45\text{ m} \times 0.31\text{ m}$) ($L \times W \times H$) was connected to an exhaust duct. The exhaust plenum kept the smoke layer interface at an elevation below all measurement points. Smoke was collected on wall mounted glass filters at two heights (54 cm and 76 cm from the base of hood).

The vertical temperature profile in the hood was measured by a thermocouple tree located at the left corner (10 cm from each wall) of the hood apparatus using 24 gauge, bare bead, K type thermocouples (not shown in Figure 1). Thirty-six thermocouples were installed on the thermocouple tree with 2.5 cm spacing. Total and radiative heat fluxes were measured using Schmidt–Boelter gauges next to each glass filter (19 cm and 14 cm from the filters as shown in Figure 1). Optical density of the layer was measured by a laser extinction measurement (wavelength 632.8 nm) across the hood at the same elevation as the glass filters (18 cm from

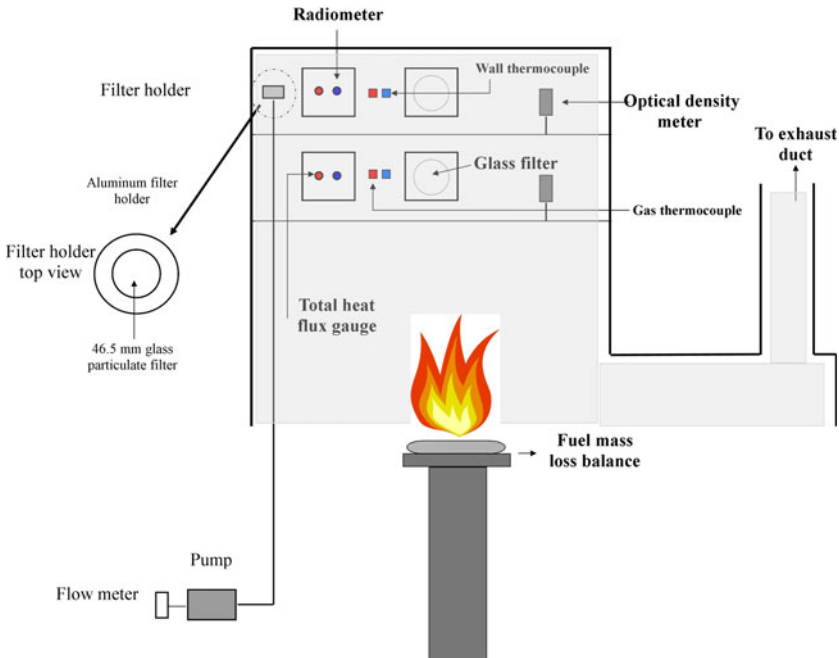


Figure 1. Front view of hood apparatus and the measurement equipment. The smoke layer is shown as the shaded region inside the hood and exhaust plenum.

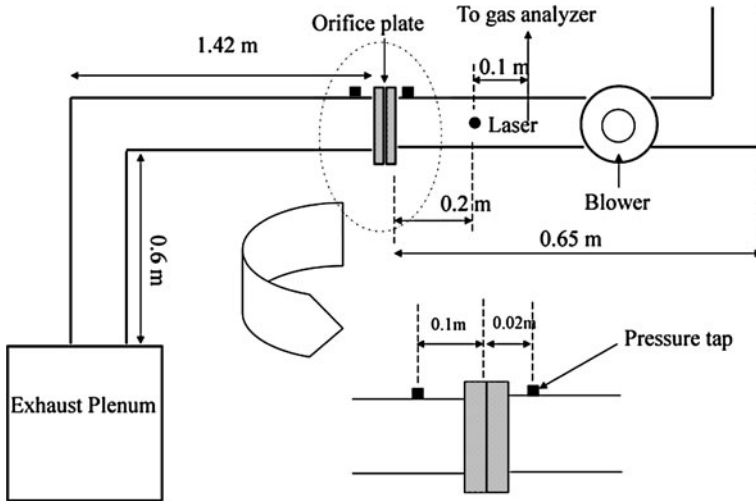


Figure 2. Exhaust flow set up and measurements.

the filters). The exhaust rate was measured using an orifice meter and the exhaust rate was controlled via blower speed control.

Figure 2 shows the exhaust duct configuration and instrumentation. Exhaust flow rate calculations were performed based on ASME PTC 19.5-2004 code [12].

Pressure difference was measured across the orifice plate at pressure taps located at 10 cm upstream and 2 cm downstream of the orifice plate. Mass loss rate for the fuel was measured by a balance with capacity of 1,000 g and 0.1 g resolution. Measurement of O_2 , CO_2 , and CO concentrations of the exhaust were made at the end of the exhaust duct. Exhaust samples were extracted (30 cm from the orifice plate as shown in Figure 2) and sent to the gas analyzers. O_2 , CO_2 , and CO concentrations were used along with the exhaust rate to calculate the heat release rate and heat of combustion.

Smoke was sampled from the hot layer at a known flow rate and used to determine the gas phase mass specific extinction coefficient. A glass particulate filter (Fischer brand filter grade G6) was placed at 76 cm above the hood base and 5 cm away from each wall in the left corner. The glass filter 42.5 mm in diameter was supported in an Aluminium filter holder (SKC, model 225-4704) as shown in Figure 1. The extraction rate of 4.6 L/min was controlled by a flow meter, which was connected to a pump. The mass of smoke collected on the pumped filter was measured at the end of each test.

3. Test Procedure

A variety of fuels, polymethylmethacrylate (PMMA), polypropylene (PP), and gasoline, was burned in the hood apparatus in order to study the smoke deposition.

These fuels have different smoke yields, and gasoline was chosen as an accelerant. In order to study the fire size effect on the smoke deposition, fuel sample sizes were varied to generate various fire sizes. Also, different fuels have different smoke yield which result in different smoke deposition. Different sample areas were used for each fuel to vary the fire size (0.09 to 3.40 kW). Test duration (1,100 to 4,500 s) was changed by increasing the thickness of the fuel samples. Sample dimensions were similar to samples used in the cone calorimeter (~ 0.1 m) so that the flames are unsteady laminar flames. For each fuel 80 tests were performed in the hood apparatus. For each test, there is a transient condition associated which is the time that the fuel sample is ignited till the flame is fully developed. The transient conditions for all the fuel are significantly short compare to the steady state conditions, except for the PP. PP needs to be converted to liquid phase first and then the flame gets fully developed.

Experimental data were collected using a National Instruments data acquisition chassis. The National Instruments hardware was interfaced with Labview 8.1 data acquisition software. The data acquisition system was set to a sampling rate of 1 Hz. Data collection was continued until the fuel sample was completely burned, all the properties were back to ambient conditions, and there was no evidence of a smoke layer in the hood apparatus.

4. Gravimetric Smoke Deposition Measurement Method

Fischer brand Grade G6 glass filters were used as smoke deposition wall targets. The diameter of the filters was 90 mm and their thickness was 0.32 mm. Glass filters were used in this research because they resist temperatures up to 600°C. Ceramic filters were evaluated but were highly susceptible to fiber mass loss, which masked the weight gain of smoke.

Glass filters were placed in the filter holders and installed on the hood wall after weighing them with the high accuracy scale (0.1 mg resolution) prior to each test. The sample line filter and wall filters were collected after each test. These filters needed to be handled carefully to assure the integrity of the gravimetric measurements. The filters were recovered when they were hot. Testing verified that there was no measurable amount of water in the sample, so the mass gain is properly interpreted as smoke deposition. The range of smoke masses found during the testing was 0.29 to 2.5 mg.

Glass filters were mounted on a sample holder constructed of inorganic fiber-board wall material (HD Duraboard) with a metal frame around it. The metal frame was made of galvanized steel with a thickness of 0.8 mm. The filters were mounted on the sample holders using 8 small pins (10 mm long) around the circumference of the filter. These pins kept the filters in place and the pins were flush to the wall material. The filter needs to be flush to the wall material in order to avoid smoke deposition on the wall material beneath the glass filter and to maintain good thermal contact of the filter with the wall material underneath the filter. The installation method is shown in Figure 3.

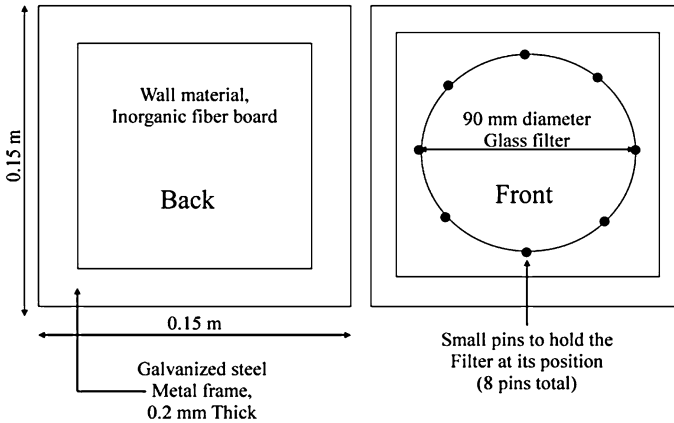


Figure 3. Front and back side of the filter holder.

5. Thermophoretic Deposition Model

Thermophoresis smoke deposition is dependent on thermophoretic velocity and smoke concentration. The thermophoretic smoke deposition velocity [13, 14] is given by:

$$V_{th} = \frac{(0.55)\eta}{\rho T} \left(\frac{dT}{dx} \right) \quad (1)$$

where η is the air viscosity and ρ and T are the air density and temperature at film temperature. Film temperature is the average between the wall and gas temperature at the location. dT/dx is the gas phase temperature gradient at the surface. The constant coefficient, 0.55, can be derived from the formulation as presented by References [15] or [16]. Measurement of the thermal gradient is discussed in detail in the data reduction section

The total amount of smoke deposited on the surface is calculated by multiplying the thermophoretic velocity V_{th} by the smoke concentration, $C_s(t)$ and integrating over the duration of the test:

$$\begin{aligned} \dot{m}'' &= V_{th}(t)C_s(t) \\ m'' &= \int_0^t V_{th}(t)C_s(t)dt \end{aligned} \quad (3)$$

6. Data Reduction

The following measurements were performed in order to calculate the thermal gradient at the surface. Total heat flux (\dot{q}_{total}'') at the level of each glass filter was

measured by using a Schmidt–Boelter heat flux gauge and radiative heat flux (\dot{q}''_{rad}) was measured by a Schmidt–Boelter radiometer. Convective heat flux (\dot{q}''_{conv}) was calculated as the difference:

$$\dot{q}''_{\text{conv}} = \dot{q}''_{\text{total}} - \dot{q}''_{\text{rad}} \quad (4)$$

Convective heat transfer coefficient (h) is given by:

$$h = \frac{\dot{q}''_{\text{total}} - \dot{q}''_{\text{rad}}}{T_{\text{gas}} - T_{\text{water}}} \quad (5)$$

in which it has been assumed that the surface temperature on the Schmidt–Boelter heat flux gauge is at the water temperature that was used to make the heat flux gauge's surface temperature constant. Water runs through the heat flux gauge and keeps the surface temperature on the gauge constant (water temperature). The average convective coefficient of heat transfer varies between 5 W/m² K and 8 W/m² K over the course of the tests. This value was calculated by averaging the data over the steady state portion of each test.

The thermal gradient can be determined by equating the convective and conductive heat flux at the surface of the heat flux gauge. k_{air} is the air conductivity at the film temperature.

$$\frac{dT}{dx} = \frac{h(T_{\text{gas}} - T_{\text{wall}})}{k_{\text{air}}} \quad (6)$$

T_{gas} and T_{wall} were measured with a set of thermocouples that were installed next to each filter. The wall thermocouple measures the surface temperature next to the filter and the gas temperature measures the gas temperature 1 inch away from the surface. The smoke was well mixed that the bulk properties of the air are being used for it except at the location very close to the wall. The temperature profile was linear from the thermocouple in the gas to wall direction which was measured for set of tests.

By replacing the convective heat transfer coefficient from Equation 5, thermal gradient is derived as follow:

$$\frac{dT}{dx} = \frac{(\dot{q}''_{\text{total}} - \dot{q}''_{\text{rad}})(T_{\text{gas}} - T_{\text{wall}})}{(T_{\text{gas}} - T_{\text{water}})k_{\text{air}}} \quad (7)$$

Measured average thermal gradients varied between 2,000 C/m and 11,000 C/m over the course of the tests. The average thermal gradient values are presented to give a representation for the thermal gradient value change and are not used in the calculations. These values were also averaged for the steady state portion of each test. Instantaneous values for the temperature gradients were used at each time step in order to calculate the thermophoretic velocity.

By employing the thermal gradient derived in Equation 7, thermophoretic velocity is determined as follows:

$$V_{th} = \frac{(0.55)\eta (\dot{q}''_{total} - \dot{q}''_{rad})(T_{gas} - T_{wall})}{\rho T (T_{gas} - T_{water})k_{air}} \quad (8)$$

Smoke deposition based on thermophoresis is the integral of the product of the thermophoretic velocity and the smoke concentration.

$$m'' = \int_0^t V_{th}(t)C_s(t)dt \quad (9)$$

Thermophoretic velocity was determined by Equation 8. Smoke concentration (C_s) can be obtained from a measurement of optical density in the hot layer:

$$C_s = \frac{OD}{\sigma_{s,g}} \quad (10)$$

where $\sigma_{s,g}$ is the gas phase mass specific extinction coefficient. By using the thermophoretic velocity equation, smoke deposition per unit area is predicted as:

$$m'' = \int_0^t \left(\frac{(0.55)\eta (\dot{q}''_{total} - \dot{q}''_{rad})(T_{gas} - T_{wall})}{\rho T (T_{gas} - T_{water})k_{air}} \right) \left(\frac{OD}{\sigma_{s,g}} \right) dt \quad (11)$$

For each test, the analytical smoke deposition prediction is compared to the gravimetric measurements on the filters.

7. Gas Phase Mass Specific Extinction Coefficient

The gas phase mass specific extinction coefficient ($\sigma_{s,g}$) was determined in each test for PMMA, gasoline, and PP. Smoke was extracted through a particulate filter at the high laser elevation (76 cm from the base of hood) using a pump at a known flow rate (4.6 L/min). Flow rate was corrected for changes in temperature between the sampling location and the flow meter. The extracted smoke was collected on a glass filter. By knowing the optical density history over the test of the smoke and measuring the mass collected on the glass filter, gas phase mass specific extinction coefficient was determined as shown in Equation 12, where m is the mass of the extracted smoke collected on the glass filter, OD is the optical density, \dot{V} is the extraction flow rate from the pump and the temperature ratio corrects for the temperature difference between the pump and the extraction point. The optical densities (extinction values) are measured by using a He-Ne laser and detector devices.

$$\sigma_{s,g} = \frac{1}{m_{collected}} \int (OD) \dot{V} \left(\frac{T_{ambient}}{T_g} \right) dt \quad (12)$$

Gas phase mass specific coefficient was determined for each test and averaged for each fuel. Table 1 shows the experimental gas phase mass specific extinction coefficient. These values were very close to gas phase mass specific coefficient values recommended by Mulholland and Croarkin [17].

8. Thermophoretic Smoke Deposition Model Validation

Surface smoke mass density data for PMMA, gasoline, and PP were compared to the predictions of the thermophoresis model. Smoke deposited on each filter was measured gravimetrically and predicted using the thermophoretic model. Eighty tests were performed for validation of the thermophoretic model. Total heat flux, radiative heat flux, gas and wall temperature, and optical density were used in the thermophoretic deposition model. Average measured $\sigma_{s,g}$ values presented in Table 1 were used. Figure 4 shows the optical density, gas and wall temperatures, and mass per unit area rate histories for a PMMA test. The mass per unit area rate has been calculated based on Equation 11.

In order to have an indication of these properties for each test, an average property will be presented for the aforementioned properties. Each property has been averaged over the test duration to give an indication for the values for each property, these averaged values are not used in the smoke deposition calculations. Figure 5 shows the same properties for a gasoline test. Test duration was 2,500 s for the PMMA test shown in Figure 4. The average temperature gradient for this test was 6,400 ($^{\circ}$ /m) which was calculated based on the heat fluxes and the gas and wall temperatures. The average optical density was 0.67 (1/m). The properties at each time step were integrated over the test duration (2,500 s) as shown in Equation 11 and the total mass per unit area was calculated (0.0047 mg/cm²).

Next figure (Figure 5) shows the same properties for the gasoline test.

The optical density history plot for a gasoline test shows a significant increase in the values from a PMMA test; however the wall and gas temperatures for the gasoline test are slightly lower than for a PMMA test.

The optical density and temperature profiles and the smoke deposition rate per unit area for PMMA and gasoline follow the same pattern. The difference in the smoke deposition is due to the difference between the smoke yields for PMMA and gasoline is reflected in the optical density plots. The temperature plot for

Table 1
Measured Gas Phase Mass Specific Extinction Coefficient for PMMA, PP, and Gasoline Tests and Comparisons with Mulholland and Croarkin [17]

	$\sigma_{s,g}$ (m ² /g) PMMA	$\sigma_{s,g}$ (m ² /g) Gasoline	$\sigma_{s,g}$ (m ² /g) PP	$\sigma_{s,g}$,Mulholland (m ² /g)
Range	7.5–8.5	7.4–8.4	7.4–8.4	7.6–9.8
Average	8.12	7.91	7.90	8.7
Standard deviation	0.29	0.31	0.29	1.1

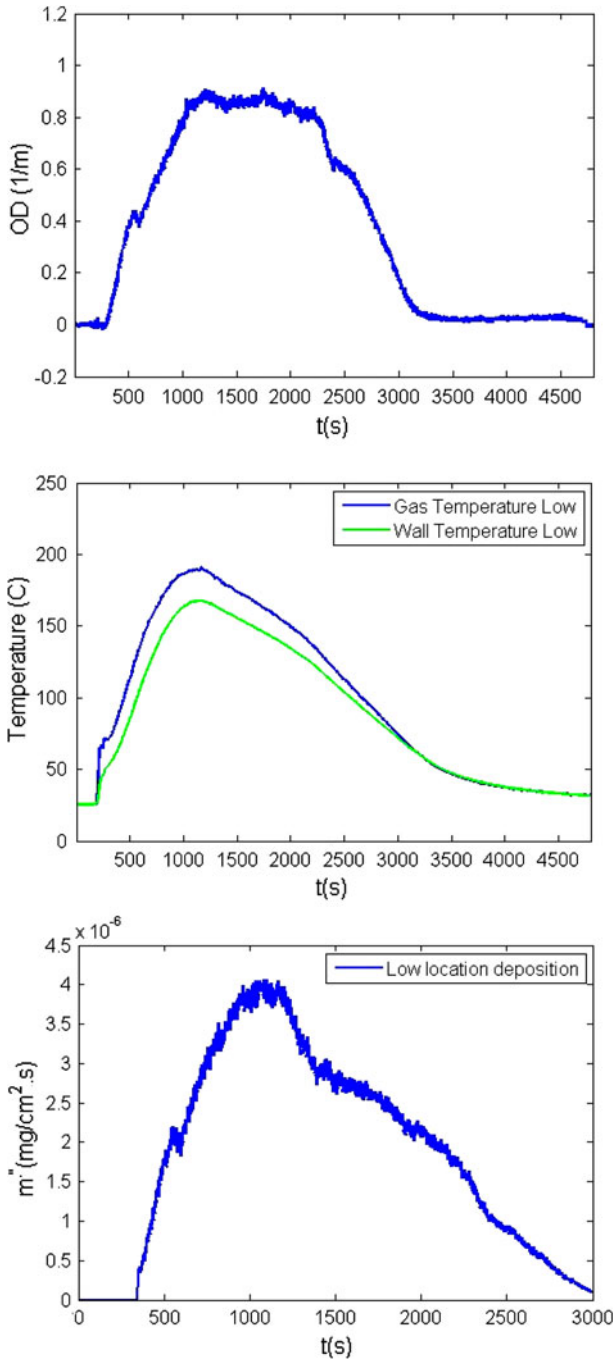


Figure 4. History plots for optical density, gas and wall temperatures, and mass per unit area rate for a PMMA test.

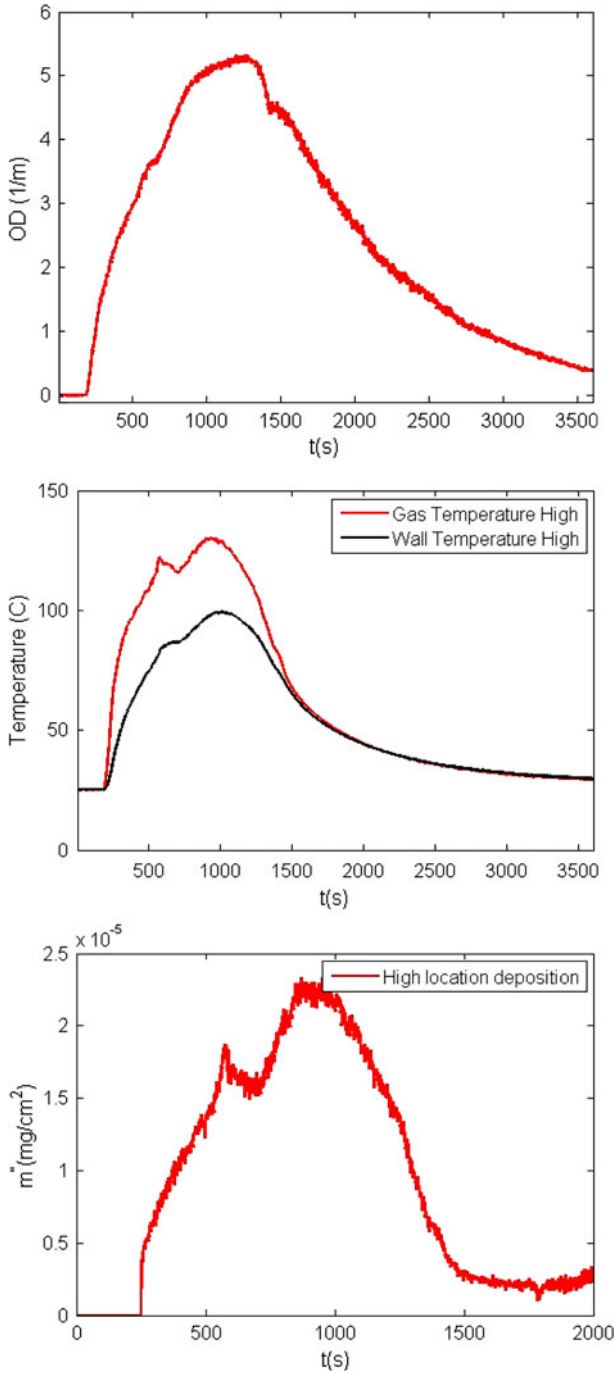


Figure 5. History plots for optical density, gas and wall temperatures, and mass per unit area rate for a gasoline test.

Gasoline shows a double peak. This is due to the ignition method which was used for Gasoline. Gasoline was burned in a 2 inch diameter cylinder. After 500 s, the flames gets to the fully developed condition and that is the reason for the jump in them temperature profile.

Figure 6 is a presentation of optical density, wall and gas temperatures, and smoke deposition per unit area rate for a PP test. Optical density plots show that the optical density is close to zero for the first 2,000 s. Polypropylene needs to be melted completely and gets into liquid phase and after that the flame for the PP test starts getting fully developed. Temperature plot shows a sudden increase in the temperature and then drop, the sudden increase is for the period which propane torch was held over the PP sample.

Figure 7 shows the predicted thermophoretic smoke deposition versus measured (gravimetric) deposition for PMMA, PP, and gasoline. $\frac{m''_{\text{predicted}}}{m''_{\text{measured}}}$ has been calculated for each data point and the averaged value for this parameter is the slope (0.98). The low and high bounds ($\pm 14\%$) in figure are calculated based on two standard deviations of $\frac{m''_{\text{predicted}}}{m''_{\text{measured}}}$. On average the model under-predicts the measurement by 2%, indicating that the thermophoretic model predicts the smoke deposition very well. This validates the thermophoretic model as an accurate model to predict smoke deposition to walls exposed to hot smoke layer environments in fires.

To provide a sense of the general importance of smoke deposition in a hot layer situation, the smoke deposition as a percentage of the total smoke produced was estimated. For all the PMMA, PP, and gasoline tests the deposition per unit rate was averaged for the low and high filter locations. This value was multiplied by the surface area of the hood apparatus to estimate the total estimated deposition. Based on measured smoke yield for each fuel and the fuel's initial mass, the total generated smoke was calculated. From the total smoke produced and the estimated total deposited smoke, the deposition percentage on the surface was estimated. Table 2 shows the range and the average values for the deposition on the surface area of the hood apparatus.

9. Conclusion

In this work gravimetric measurements of smoke deposition on walls were successfully made using glass filters mounted on the wall surface. Predictions of thermophoretic smoke deposition were made through measurement of smoke concentration and thermal gradient at the wall surface. The thermophoretic model successfully predicted the gravimetrically measured smoke deposition on the walls exposed to a hot smoky layer. In our prior investigation of fires against walls, the thermophoretic smoke deposition model successfully predicted wall smoke deposition due to an exposing fire source [9]. The present work and the prior work [9] show that thermophoresis is the dominant smoke deposition mechanisms for wall surfaces in fire, whether the fire is directly against the wall or the wall is exposed to a hot, smoky layer. For high wall temperatures smoke oxidation needs to be considered [18]. Other smoke deposition mechanisms are expected to contribute to

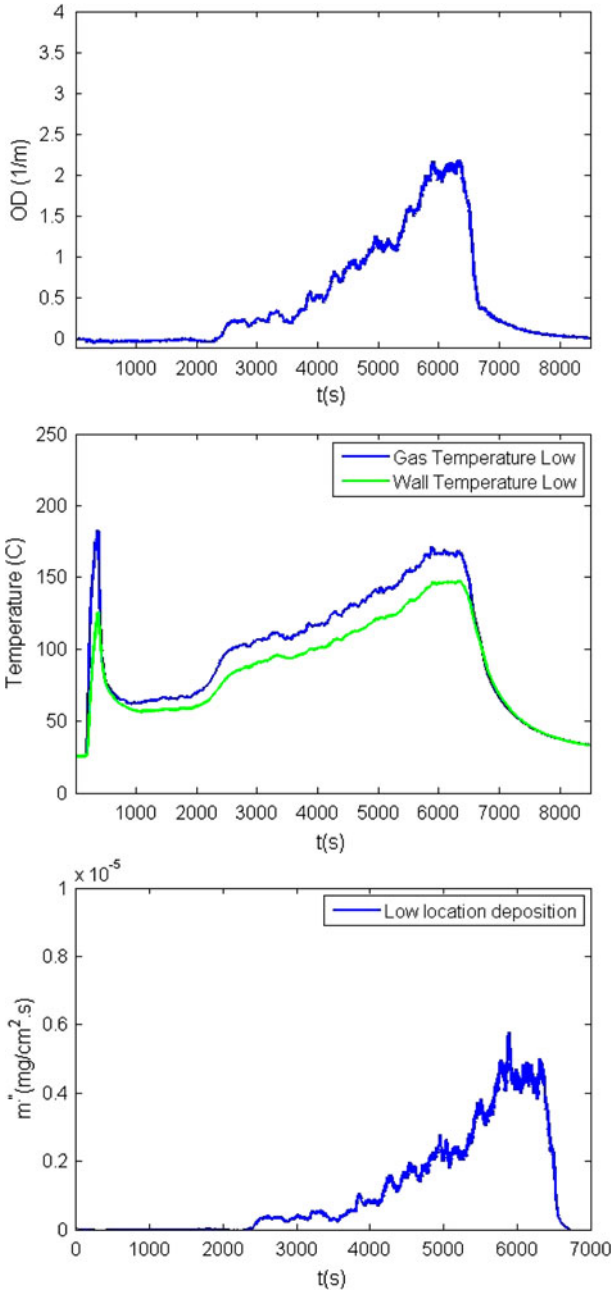


Figure 6. History plots for optical density, gas and wall temperatures, and mass per unit area rate for a PP test.

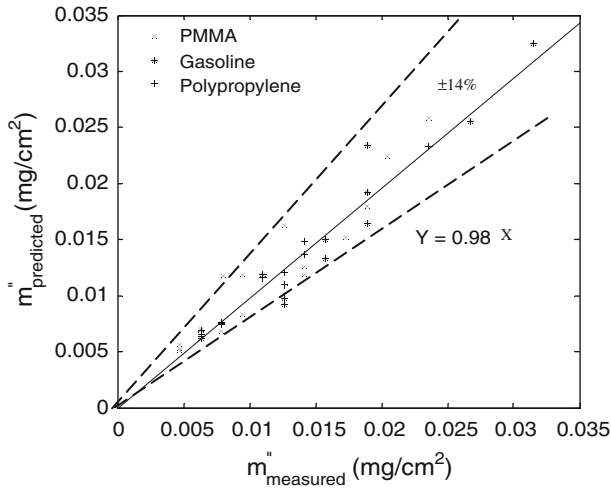


Figure 7. Predicted thermophoretic deposition versus measured (gravimetric) deposition for PMMA, PP, and gasoline experiments.

**Table 2
Calculated Smoke Deposition Percentage on the Hood Apparatus Surface for PMMA, PP, and Gasoline**

	PMMA (%)	PP (%)	Gasoline (%)
Range	6.6–15.1	1.8–5.9	6.0–15.0
Average	9.2	2.8	10.7

floor and ceiling surfaces. Additional research is required for these surface orientations.

Optical smoke properties were measured for PMMA, PP, and gasoline. These results were in agreement with the values recommended by Mulholland and Croarkin [17].

References

- Butler K, Mulholland G (2004) Generation and transport of smoke components. *Fire Technol* 40(2):149–176. doi:[10.1023/B:FIRE.0000016841.07530.64](https://doi.org/10.1023/B:FIRE.0000016841.07530.64)
- Mulholland GW (2002) Smoke production and properties, The SFPE handbook of fire protection engineering. National Fire Protection Association, Quincy, pp. 258–268
- Ciro W, Eddings E, Sarofim A (2006) Experimental and numerical investigation of transient soot buildup on a cylindrical container immersed in a jet fuel pool fire. *Combust Sci Technol* 178(12):2199–2218. doi:[10.1080/00102200600626108](https://doi.org/10.1080/00102200600626108)
- Sippola MR, Nazaroff WW (2005) Particle deposition in ventilation ducts: connectors, bends and developing turbulent flow. *Aerosol Sci Technol* 39:139–150. doi:[10.1080/027868290908759](https://doi.org/10.1080/027868290908759)

5. Guha A (1997) A unified Eulerian theory of turbulent deposition to smooth and rough surfaces. *J Aerosol Sci* 28:1517–1537. doi:[10.1016/S0021-8502\(97\)00028-1](https://doi.org/10.1016/S0021-8502(97)00028-1)
6. Gottuk D, Mealy C, Floyd J (2009) Smoke transport and FDS validation. *Fire Saf Sci* 9:129–140. doi:[10.3801/IAFSS.FSS.9-129](https://doi.org/10.3801/IAFSS.FSS.9-129)
7. Hamins A, Maranghides A, Johnsson EL, Donnelly MK, Yang JC, Mulholland GW, Anleitner RL (2005) Report of experimental results for the international fire model benchmarking and validation exercise #3. National Institute of Standards and Technology, Gaithersburg
8. Floyd J (2010) Modeling soot deposition using large eddy simulation with a mixture fraction based framework, Interflam 2010. Interscience Communications, London
9. Riahi S, Beyler C (2011) Measurement and prediction of smoke deposition from a fire against a wall. *Fire Saf Sci* 10:641–654. doi:[10.3801/IAFSS.FSS.10-641](https://doi.org/10.3801/IAFSS.FSS.10-641)
10. Riahi S (2010) New tools for smoke residue and deposition analysis. PhD Dissertation, Department of Civil and Environmental Engineering, The George Washington University, Washington DC
11. Properties for the duraboard Fiberfrax from <http://www.fiberfrax.com/>. Accessed 24 may 2012
12. ASTM (2004) PTC. 19.5 Flow Measurement
13. Talbot L, Cheng R, Schefer R, Willis D (2006) Thermophoresis of particles in a heated boundary layer. *J Fluid Mech* 101(04):737. doi:[10.1017/S0022112080001905](https://doi.org/10.1017/S0022112080001905)
14. Waldmann L, Schmitt K (1966) *Aerosol science*. Academic Press, New York
15. Brock J (1962) On the theory of thermal forces acting on aerosol particles. *J Colloid Sci* 17(8):768–780. doi:[10.1016/0095-8522\(62\)90051-X](https://doi.org/10.1016/0095-8522(62)90051-X)
16. Friedlander S (2000) *Smoke, dust, and haze: fundamentals of aerosol dynamics*. Oxford University Press, New York
17. Mulholland GW, Croarkin C (2000) Specific extinction coefficient of flame generated smoke. *Fire Mater* 24:227–230. doi:[10.1002/1099-1018\(200009/10\)24:5<227::AID-FAM742>3.0.CO;2-9](https://doi.org/10.1002/1099-1018(200009/10)24:5<227::AID-FAM742>3.0.CO;2-9)
18. Hartman JR, Beyler AP, Riahi S, Beyler CL (2011) Smoke oxidation kinetics for application to prediction of clean burn patterns. *Fire Mater* . doi:[10.1002/fam.1099](https://doi.org/10.1002/fam.1099)